



Wearable Thermocells Based on Gel Electrolytes for the Utilization of Body Heat

Peihua Yang⁺, Kang Liu⁺, Qian Chen, Xiaobao Mo, Yishu Zhou, Song Li, Guang Feng, and Jun Zhou*

Abstract: Converting body heat into electricity is a promising strategy for supplying power to wearable electronics. To avoid the limitations of traditional solid-state thermoelectric materials, such as fragility and complex fabrication processes, we fabricated two types of thermogalvanic gel electrolytes with positive and negative thermo-electrochemical Seebeck coefficients, respectively, which correspond to the *n*-type and *p*-type elements of a conventional thermoelectric generator. Such gel electrolytes exhibit not only moderate thermoelectric performance but also good mechanical properties. Based on these electrolytes, a flexible and wearable thermocell was designed with an output voltage approaching 1 V by utilizing body heat. This work may offer a new train of thought for the development of self-powered wearable systems by harvesting low-grade body heat.

Given the recent developments in the area of wearable electronics and e-skins,^[1–6] the emerging need for self-powered energy supply has heightened the interest in energy harvesting from the environment or human beings. Among recognized energy-harvesting technologies, such as solar cells^[7,8] and triboelectric and electret generators,^[9,10] thermal energy is a potential power source that is widely available in the environment and in industrial processes.^[11,12] However, human bodies are also a permanent heat source, with a surface temperature of about 32 °C and possibly tens of degrees temperature difference between the human body and its environment.^[13,14] Hence, it is of practical meaning to convert body heat energy, a type of low-grade heat, into electricity for directly powering wearable electronics.^[15–17]

The most convenient strategy to utilize low-grade heat is thermal–electric conversion. Traditional thermoelectric generators utilizing the Seebeck effect are mainly based on solid-state semiconductors or conducting polymers,^[18,19] with output voltages limited by the relatively low Seebeck

coefficient (several hundreds μVK^{-1}). Meanwhile, the fragility and expensiveness of thermoelectric materials as well as their complicated fabrication processes are other obstacles restricting their application in wearable electronics.^[20] Alternatively, a large thermovoltage can be derived from thermogalvanic effects, resulting from temperature-dependent entropy changes during electron transfer between redox couples and electrodes.^[21–24] Previous reports mainly focused on the exploration of electrode materials, such as carbon nanotubes (CNTs) and graphene,^[25–28] to achieve high thermal–electric conversion efficiencies. However, because of the aqueous electrolytes used in thermocells, large-scale integration and packaging of the units would be more difficult in applications, especially for wearable devices.^[29] Inspired by the successful application of gel electrolytes in solid-state electrochemical energy storage systems and stretchable ionic conductors,^[30–33] we surmised that solid-state or quasi-solid-state gel electrolytes may enable the large-scale integration of thermocells.

Herein, we report an integrated wearable thermocell based on gel electrolytes for low-grade thermal energy conversion. Poly(vinyl alcohol) (PVA) was used as the gel solution, with addition of ferric/ferrous chloride or potassium ferricyanide/ferrocyanide couples to obtain thermogalvanic gel electrolytes exhibiting positive or negative thermo-electrochemical Seebeck coefficients. The prepared PVA/ferric/ferrous chloride and PVA/potassium ferricyanide/ferrocyanide gel electrolytes are denoted as PFC and PPF, respectively. As illustrated in Scheme 1, the integrated device was designed by connecting the PFC and PPF units sequentially in series, with alternating top and bottom interconnections. The integrated wearable device can generate an open-circuit voltage of about 0.7 V and a short-circuit current of approximately 2 μA by utilizing body heat, achieving a maximum output power of about 0.3 μW .

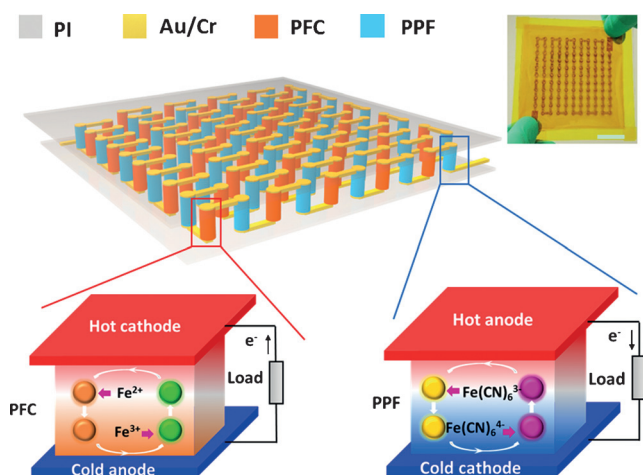
The detailed fabrication process of the thermogalvanic gels is discussed in the Supporting Information. When a laser transits through the produced gels, distinct light scattering is observed (known as the Tyndall effect),^[34] indicating the homogeneity of the gels (Figure 1a). In contrast to the liquidity of aqueous electrolytes, the as-prepared quasi-solid-state thermogalvanic gels exhibit good moldability and can be made into films with significant mechanical strength (Figure 1b). The specified samples (ca. 15 mm \times 8 mm \times 1 mm) had sufficient mechanical strength up to 0.1 MPa. Simultaneously, the tensile properties of the gels are also remarkable as they can be stretched to 2–4 times their original length. All of these outstanding mechanical properties are beneficial for the application of these gels in wearable electronic systems.

[*] P. Yang,^[†] Dr. K. Liu,^[†] Q. Chen, Dr. X. Mo, Y. Zhou, Prof. J. Zhou
Wuhan National Laboratory for Optoelectronics
School of Optical and Electronic Information
Huazhong University of Science and Technology
Wuhan 430074, Hubei (China)
E-mail: jun.zhou@mail.hust.edu.cn

Prof. S. Li, Prof. G. Feng
State Key Laboratory of Coal Combustion
School of Energy and Power Engineering
Huazhong University of Science and Technology
Wuhan 430074, Hubei (China)

[†] These authors contributed equally to this work.

Supporting information for this article can be found under:
<http://dx.doi.org/10.1002/anie.201606314>.



Scheme 1. The integrated gel-based thermocell. Both the PFC and PPF gels were sandwiched between two flexible substrates (polyimide, PI). With alternating top and bottom interconnections, the PFC and PPF gels are connected sequentially in series. The magnified insets illustrate the operation mechanism of the gel-based thermocell. At a certain temperature difference, the thermo-voltage polarity of PFC and PPF is exactly reversed. The top right inset is a photograph of the integrated device (scale bar: 2 cm).

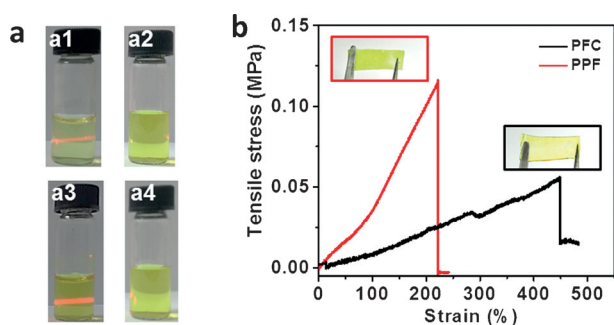


Figure 1. Physical state and mechanical performance of the thermogalvanic gels. a) Photographs of laser-irradiated samples of a1) a PFC gel, a2) aqueous $\text{FeCl}_2/\text{FeCl}_3$, a3) a PPF gel, and a4) aqueous $\text{K}_4\text{Fe}(\text{CN})_6/\text{K}_3\text{Fe}(\text{CN})_6$. b) Stress-strain curves for PFC and PPF gel films. The tests were carried out at a stretching rate of 5 mm min^{-1} (at ca. 23°C and a relative humidity (RH) of ca. 65%). Insets: Photographs of films made from PFC and PPF gels.

The thermo-electrochemical Seebeck coefficients of the pure $\text{Fe}^{2+}/\text{Fe}^{3+}$ and $\text{Fe}(\text{CN})_6^{4-}/\text{Fe}(\text{CN})_6^{3-}$ thermogalvanic couples are around 1 mV K^{-1} in aqueous solution.^[35] The mechanism of thermovoltage generation from PFC and PPF gels is similar to that of pure $\text{Fe}^{2+}/\text{Fe}^{3+}$ and $\text{Fe}(\text{CN})_6^{4-}/\text{Fe}(\text{CN})_6^{3-}$, in which charges are transferred by the migration of ions through electrolytes under a temperature difference rather than only by the migration of carriers (electrons or holes) through the semiconductor thermocouple, as illustrated in Scheme 1. Electrons, released by the oxidation process ($\text{Fe}^{2+} - e \rightarrow \text{Fe}^{3+}$ or $\text{Fe}(\text{CN})_6^{4-} - e \rightarrow \text{Fe}(\text{CN})_6^{3-}$) at the anode, pass through an external load injected to the cathode by reduction ($\text{Fe}^{3+} + e \rightarrow \text{Fe}^{2+}$ or $\text{Fe}(\text{CN})_6^{3-} + e \rightarrow \text{Fe}(\text{CN})_6^{4-}$). At a certain temperature difference, the hot end of the PFC is the cathode, and the PPF is the anode. Figure 2a describes the

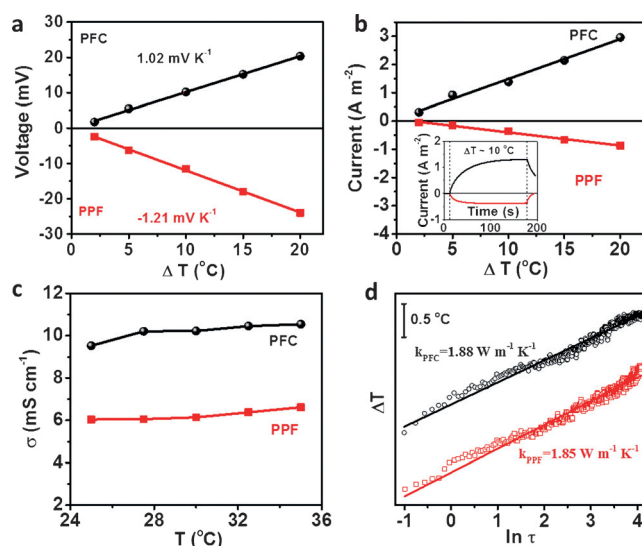


Figure 2. Thermogalvanic performance of independent PFC and PPF gels. a) Dependence of the thermo-voltage on the temperature difference. b) The short-circuit current as a function of the temperature difference. The distance between the hot and cold ends was 1 mm, and each electrode was 3 mm in diameter. The temperatures of the cold and hot ends were controlled by circulating water and with an electrical heating plate, respectively. The inset in (b) shows the current response at a temperature difference of about 10°C . c) Electrical conductivities of the thermogalvanic gels at different temperatures. d) Thermal conductivities of the thermogalvanic gels at room temperature (ca. 23°C).

thermovoltage response of PFC and PPF gels at various temperature differences for a device thickness of 1 mm and with Au/Cr as the electrodes. The thermo-electrochemical Seebeck coefficients of PFC and PPF are 1.02 and -1.21 mV K^{-1} , respectively, close to the values of aqueous electrolytes. Similar to n-type and p-type solid-state thermo-electric semiconductors, the opposite signs of the thermo-electrochemical Seebeck coefficients of the PFC and PPF gels play an important role in an integrated thermocell as demonstrated below.

The generated current is proportional to the temperature difference between the two ends. Figure 2b shows the current response of the gels under various temperature differences, and the current increases linearly with an increase in temperature difference. At a specific temperature difference of $\Delta T \approx 10^\circ\text{C}$, the PPF sample exhibits a current density of 0.4 A m^{-2} whereas the PFC sample generates a steady current density of about 1.3 A m^{-2} . When the heating source is removed, the current immediately drops. This current density is a little bit lower than that of thermocells based on aqueous electrolytes. Figure 2c shows the electrical conductivities of the PPF and PFC gels at different temperatures (carefully analyzed in the Supporting Information, Figure S1). Similar to redox-free polymer electrolytes,^[36] the electrical conductivities of PPF and PFC gels slightly increase as the temperature increases, but retain their order of magnitude of 10 mS cm^{-1} , which is quite a bit smaller than those of aqueous electrolytes (600 mS cm^{-1}),^[37] but comparable to those of proton-conducting polymer electrolytes (ca. 10 mS cm^{-1})^[38]

and much higher than those of solid-state LiPON electrolytes ($1.02 \times 10^{-3} \text{ mS cm}^{-1}$).^[39]

The thermal conductivities of the gels shown in Figure 2d were measured by the transient hot-wire method,^[40] which gave values of about 1.88 and 1.85 $\text{W m}^{-1} \text{K}^{-1}$ for the PFC and PPF gels, respectively. Although these gels show higher thermal conductivity than aqueous solutions (ca. $0.6 \text{ W m}^{-1} \text{K}^{-1}$),^[41] their heat transfer capacity is actually lower because of the large heat convection in aqueous solutions ($200\text{--}1000 \text{ W m}^{-2} \text{K}^{-1}$ for natural convection). Thus it is easier to build up an effective temperature difference along the quasi-solid-state gels for constructing a more compact electricity generation device than to use aqueous-electrolyte-based thermogalvanic systems.

The quasi-solid-state thermogalvanic gels can be molded into different shapes, which is beneficial for integration and packaging. To achieve large-scale integration of the thermocells, we studied the performance of one PFC device and one PPF device connected in series as shown in Figure 3a. Here,

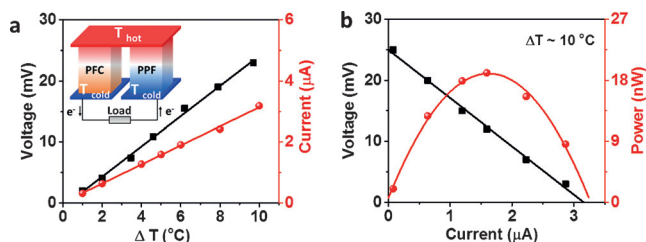


Figure 3. The thermogalvanic performance of a PFC cell and a PPF cell connected in series by using a Au/Cr electrode. a) Voltage and current as a function of the temperature difference. The inset is a schematic representation of the two types of cells connected in series, with the hot and cold ends on the same side. b) The dependence of the steady-state voltage and output power on the current at a temperature difference of approximately 10°C .

we used two units of PFC and PPF gels to construct a tandem device (Au/Cr as the electrodes). The output voltage and current increase linearly with an increase in the temperature difference. At a temperature difference of about 10°C , the output voltage of the tandem device is almost twice the value of the individual ones (ca. 23 mV) while the current hardly changes (ca. $3 \mu\text{A}$) owing to the limitations of PPF. The corresponding voltage and power outputs of the series-connected generator as a function of the current under steady-state conditions are given in Figure 3b. The maximum output power (P_{max}) is approximately 19 nW, which can be enhanced by increasing the temperature difference, achieving nearly 90 nW at $\Delta T \approx 20^\circ\text{C}$ (Figure S2).

To demonstrate the potential applications of the thermogalvanic gels in wearable systems, we fabricated an integrated device containing 59 PFC and 59 PPF gel units (1 mm in height and 3 mm in diameter), with bridging Au/Cr interconnections on flexible PI substrate as illustrated in the inset in Scheme 1. As expected, the generated voltage of the device increased linearly with the temperature difference, and can reach 0.85 V at an applied temperature difference of about 12°C (Figure S3). The average thermo-electrochemical See-

beck coefficient was calculated to be 0.6 mVK^{-1} , which is lower than the measured values of 1.02 mVK^{-1} for PFC and 1.21 mVK^{-1} for PPF, which may be due to the thermal contact resistance between the gels and substrates.

Human bodies are a natural heat source and have great potential for directly powering wearable electronics by utilizing the temperature difference between human bodies and their environment. When the integrated device is put on a hand as shown in Figure 4a, an open-circuit voltage of about

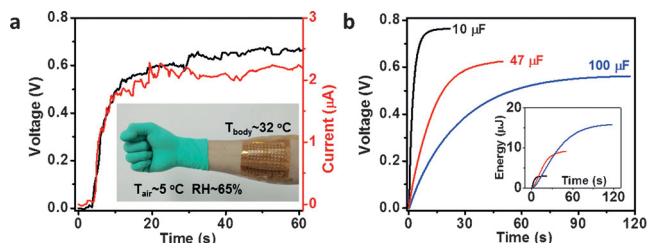


Figure 4. Applications of the wearable thermocell. a) The voltage and current generated by the thermocell from body heat. The inset shows a photograph of the wearable thermocell on a hand. b) Voltage–time curves of different capacitors charged by the thermocell utilizing human body heat. The inset shows the energy stored in the capacitors, which is also the electrical energy harvested from the body heat.

0.7 V and a short-circuit current of approximately $2 \mu\text{A}$ were generated at an ambient temperature of 5°C . The maximum output power was about $0.3 \mu\text{W}$, which is much higher than that of wearable transition-metal dichalcogenide integrated thermoelectric generators (7.3 nW making use of body heat),^[13] and comparable to the $(\text{Bi,Sb})_2\text{Te}_3$ thermoelectric elements in MEMS (ca. $1 \mu\text{W}$ under lamp illumination).^[42] It should be noted that the generated voltage is much lower than expected (1.9 V for the temperature difference between a body surface of ca. 32°C and an ambient temperature of 5°C based on the average thermo-electrochemical Seebeck coefficient), implying that the temperature difference established along the gels is much smaller than predicted. Hence the output voltage could be further enhanced by systematic optimization.^[43] In the meantime, the generated current could be effectively promoted by employing electrode materials such as CNT forest and aerogels.^[25,26] The electricity generated by our thermogalvanic generator can be directly utilized or stored in capacitors. As shown in Figure 4b, a $10 \mu\text{F}$ capacitor can be charged to about 0.7 V in 15 s, and a $100 \mu\text{F}$ capacitor can be charged to approximately 0.55 V within 120 s by our integrated thermogalvanic generator by utilizing body heat.

In summary, we have fabricated two types of thermogalvanic gel electrolytes, exhibiting outstanding mechanical properties and comparable thermoelectric performance to aqueous thermogalvanic electrolytes. The quasi-solid-state thermogalvanic gel electrolytes can be easily molded into different shapes for facile integration and packaging. Based on these properties, a proof-of-concept wearable thermocell was developed for harvesting body heat energy. This work may open up new prospects for both thermocells and wearable functional electronics.

Acknowledgements

This work was financially supported by the National Natural Science Foundation of China (51322210 and 61434001), the National Program for Support of Top-Notch Young Professionals, the China Postdoctoral Science Foundation (2015M570639), the Fundamental Research Funds for the Central Universities (HUST: 2015MS004), and the Director Fund of WNLO. We acknowledge facility support of the Center for Nanoscale Characterization & Devices, WNLO-HUST and the Analysis and Testing Center of Huazhong University of Science and Technology.

Keywords: flexible electronics · gel electrolytes · thermoelectric materials · thermocells · wearable electronics

How to cite: *Angew. Chem. Int. Ed.* **2016**, *55*, 12050–12053
Angew. Chem. **2016**, *128*, 12229–12232

- [1] W. Gao, S. Emaminejad, H. Y. Y. Nyein, S. Challa, K. Chen, A. Peck, H. M. Fahad, H. Ota, H. Shiraki, D. Kiriya, D.-H. Lien, G. A. Brooks, R. W. Davis, A. Javey, *Nature* **2016**, *529*, 509.
- [2] J. Kim, D. Son, M. Lee, C. Song, J.-K. Song, J. H. Koo, D. J. Lee, H. J. Shim, J. H. Kim, M. Lee, T. Hyeon, D.-H. Kim, *Sci. Adv.* **2016**, *2*, e1501101.
- [3] A. Chortos, Z. Bao, *Mater. Today* **2014**, *17*, 321.
- [4] J. Song, J. Li, J. Xu, H. Zeng, *Nano Lett.* **2014**, *14*, 6298.
- [5] T. Chen, L. Qiu, H. G. Kia, Z. Yang, H. Peng, *Adv. Mater.* **2012**, *24*, 4623.
- [6] J. Ren, W. Bai, G. Guan, Y. Zhang, H. Peng, *Adv. Mater.* **2013**, *25*, 5965.
- [7] S. Pan, Z. Yang, P. Chen, J. Deng, H. Li, H. Peng, *Angew. Chem. Int. Ed.* **2014**, *53*, 6110; *Angew. Chem.* **2014**, *126*, 6224.
- [8] T. Chen, L. Qiu, Z. Cai, F. Gong, Z. Yang, Z. Wang, H. Peng, *Nano Lett.* **2012**, *12*, 2568.
- [9] Z. L. Wang, *ACS Nano* **2013**, *7*, 9533.
- [10] Q. Zhong, J. Zhong, B. Hu, Q. Hu, J. Zhou, Z. L. Wang, *Energy Environ. Sci.* **2013**, *6*, 1779.
- [11] J. R. Sootsman, D. Y. Chung, M. G. Kanatzidis, *Angew. Chem. Int. Ed.* **2009**, *48*, 8616; *Angew. Chem.* **2009**, *121*, 8768.
- [12] W. G. Zeier, A. Zevalkink, Z. M. Gibbs, G. Hautier, M. G. Kanatzidis, G. J. Snyder, *Angew. Chem. Int. Ed.* **2016**, *55*, 6826; *Angew. Chem.* **2016**, *128*, 6938.
- [13] J. Y. Oh, J. H. Lee, S. W. Han, S. S. Chae, E. J. Bae, Y. H. Kang, W. J. Choi, S. Y. Cho, J.-O. Lee, H. K. Baik, T. I. Lee, *Energy Environ. Sci.* **2016**, *9*, 1696.
- [14] J. Zhong, Y. Zhang, Q. Zhong, Q. Hu, B. Hu, Z. L. Wang, J. Zhou, *ACS Nano* **2014**, *8*, 6273.
- [15] V. Leonov, T. Torfs, P. Fiorini, C. V. Hoof, *IEEE Sens. J.* **2007**, *7*, 650.
- [16] F. Suarez, A. Nozariasbmarz, D. Vashaee, M. C. Öztürk, *Energy Environ. Sci.* **2016**, *9*, 2099.
- [17] S. J. Kim, J. H. We, B. J. Cho, *Energy Environ. Sci.* **2014**, *7*, 1959.
- [18] G. J. Snyder, E. S. Toberer, *Nat. Mater.* **2008**, *7*, 105.
- [19] Z. U. Khan, J. Edberg, M. M. Hamed, R. Gabrielson, H. Granberg, L. Wågberg, I. Engquist, M. Berggren, X. Crispin, *Adv. Mater.* **2016**, *28*, 4556.
- [20] S. K. Bux, J.-P. Fleurial, R. B. Kaner, *Chem. Commun.* **2010**, *46*, 8311.
- [21] T. I. Quickenden, C. F. Vernon, *Sol. Energy* **1986**, *36*, 63.
- [22] Y. V. Kuzminskii, V. A. Zasukha, G. Y. Kuzminskaya, *J. Power Sources* **1994**, *52*, 231.
- [23] A. V. Sokirko, *Electrochim. Acta* **1994**, *39*, 597.
- [24] J. Newman, *Ind. Eng. Chem. Res.* **1995**, *34*, 3208.
- [25] R. Hu, B. A. Cola, N. Haram, J. N. Barisci, S. Lee, S. Stoughton, G. Wallace, C. Too, M. Thomas, A. Gestos, M. E. dela Cruz, J. P. Ferraris, A. A. Zakhidov, R. H. Baughman, *Nano Lett.* **2010**, *10*, 838.
- [26] H. Im, T. Kim, H. Song, J. Choi, J. S. Park, R. Ovalle-Robles, H. D. Yang, K. D. Kihm, R. H. Baughman, H. H. Lee, T. J. Kang, Y. H. Kim, *Nat. Commun.* **2016**, *7*, 10600.
- [27] T. J. Kang, S. Fang, M. E. Kozlov, C. S. Haines, N. Li, Y. H. Kim, Y. Chen, R. H. Baughman, *Adv. Funct. Mater.* **2012**, *22*, 477.
- [28] M. S. Romano, N. Li, D. Antiohos, J. M. Razal, A. Nattestad, S. Beirne, S. Fang, Y. Chen, R. Jalili, G. G. Wallace, R. Baughman, J. Chen, *Adv. Mater.* **2013**, *25*, 6602.
- [29] H. Im, H. Moon, J. Lee, I. Chung, T. Kang, Y. Kim, *Nano Res.* **2014**, *7*, 443.
- [30] X. Peng, H. Liu, Q. Yin, J. Wu, P. Chen, G. Zhang, G. Liu, C. Wu, Y. Xie, *Nat. Commun.* **2016**, *7*, 11782.
- [31] X. Xiao, T. Q. Li, Z. H. Peng, H. Y. Jin, Q. Z. Zhong, Q. Y. Hu, B. Yao, Q. P. Luo, C. F. Zhang, L. Gong, J. Chen, Y. Gogotsi, J. Zhou, *Nano Energy* **2014**, *6*, 1.
- [32] Y. Xu, Y. Zhao, J. Ren, Y. Zhang, H. Peng, *Angew. Chem. Int. Ed.* **2016**, *55*, 7979; *Angew. Chem.* **2016**, *128*, 8111.
- [33] C. Keplinger, J.-Y. Sun, C. C. Foo, P. Rothmund, G. M. Whitesides, Z. Suo, *Science* **2013**, *341*, 984.
- [34] Y. Li, B. P. Bastakoti, V. Malgras, C. Li, J. Tang, J. H. Kim, Y. Yamauchi, *Angew. Chem. Int. Ed.* **2015**, *54*, 11073; *Angew. Chem.* **2015**, *127*, 11225.
- [35] T. I. Quickenden, Y. Mua, *J. Electrochem. Soc.* **1995**, *142*, 3985.
- [36] D. Zhao, H. Wang, Z. U. Khan, J. C. Chen, R. Gabrielson, M. P. Jonsson, M. Berggren, X. Crispin, *Energy Environ. Sci.* **2016**, *9*, 1450.
- [37] N. S. Hudak, G. G. Amatucci, *J. Electrochem. Soc.* **2011**, *158*, A572.
- [38] M. Rikukawa, K. Sanui, *Prog. Polym. Sci.* **2000**, *25*, 1463.
- [39] H.-K. Kim, S.-H. Cho, O. Young-Woo, T.-Y. Seong, Y. S. Yoon, *J. Vac. Sci. Technol. B* **2003**, *21*, 949.
- [40] Y. Nagasaka, A. Nagashima, *J. Phys. E* **1981**, *14*, 1435.
- [41] M. S. Romano, S. Gambhir, J. M. Razal, A. Gestos, G. G. Wallace, J. Chen, *J. Therm. Anal. Calorim.* **2012**, *109*, 1229.
- [42] G. J. Snyder, J. R. Lim, C.-K. Huang, J.-P. Fleurial, *Nat. Mater.* **2003**, *2*, 528.
- [43] M. Lossec, B. Multon, H. Ben Ahmed, *Energy Convers. Manage.* **2013**, *68*, 260.

Received: June 29, 2016

Published online: August 25, 2016